Electronic Supplementary Information

Bifunctional $NiCuO_x$ photoelectrodes to promote pseudocapacitive charge storage by *in-situ* photocharging

Ting Zhu [acd]*, *Jun Pan,* [b] *Zhiyu An,* [b] *Rongjie Zhe,* [a]
Quanhong Ou, [a] *and Hong-En Wang* [acd]*

[a] School of Physics and Electronic Information, Yunnan Normal University, 768 Juxian Street, Kunming 650500, Yunnan, China.

[b] School of Materials Science and Engineering, Central South University, 932 Lushan Road South, Changsha 410083, Hunan, China.

[c] Yunnan Key Laboratory of Optoelectronic Information Technology, School of Physics and Electronic Information, Yunnan Normal University, Kunming 650500, China.

[d] Key Laboratory of Advanced Technique & Preparation for Renewable Energy Materials, Ministry of Education, Yunnan Normal University, Kunming 650500, China.

*Email: zhut0002@ynnu.edu.cn (T. Zhu); hongen.wang@outlook.com (H. E. Wang)

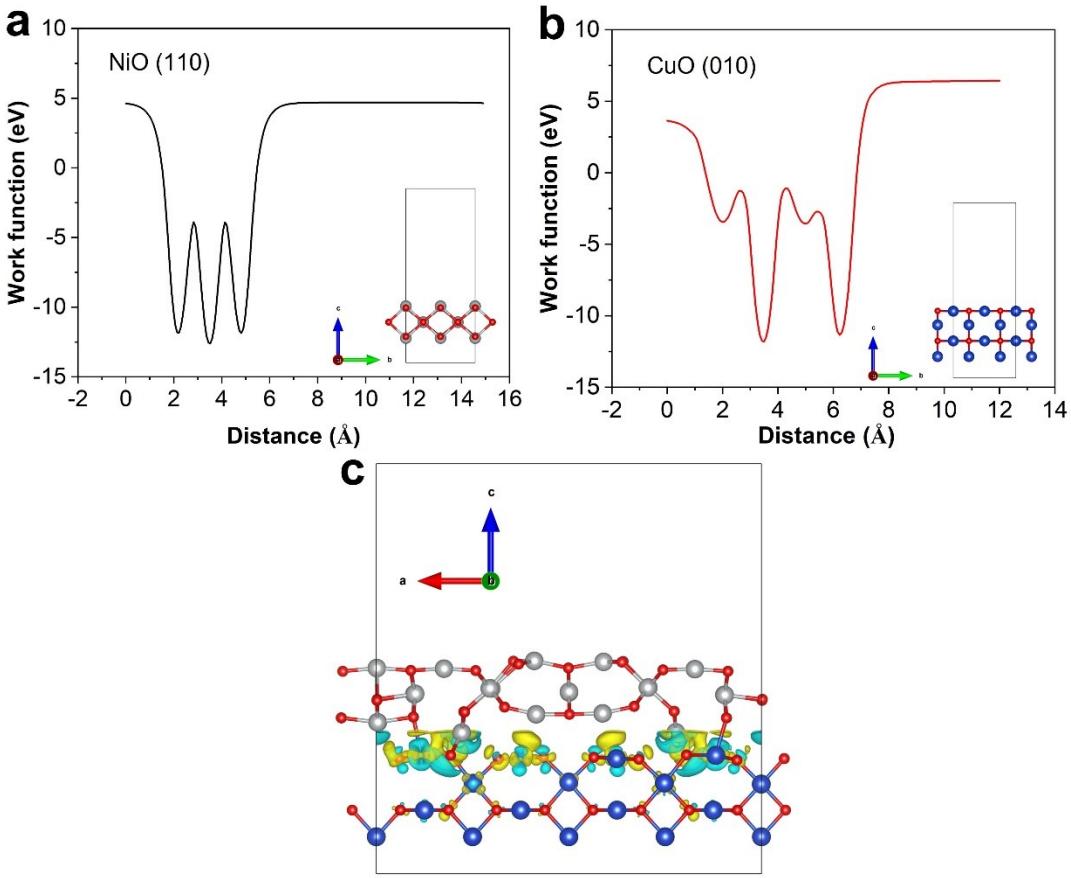

Fig. S1 Calculated work functions (a and b) of NiO (110) and CuO (010), and charge density distribution contour (c) of the NiO-CuO interface.

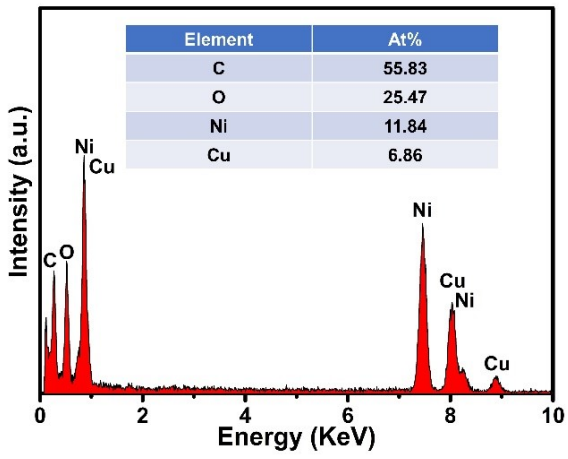

Fig. S2 EDS results of the sample CC@NiCuO$_x$.

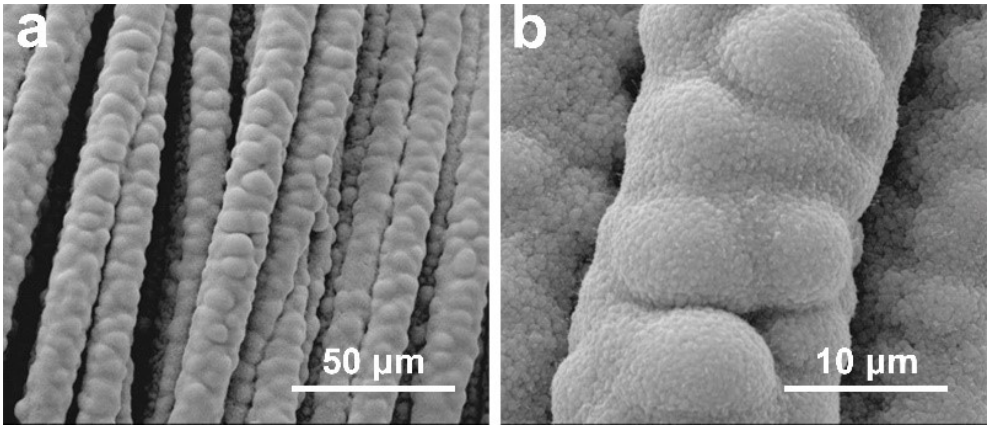

Fig. S3 SEM images of the CC@CuO_x.

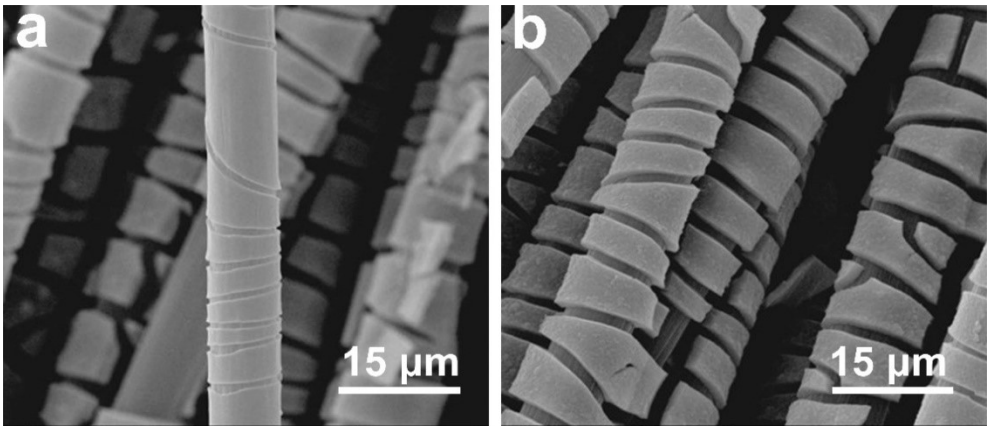

Fig. S4 SEM images of the CC@NiO.

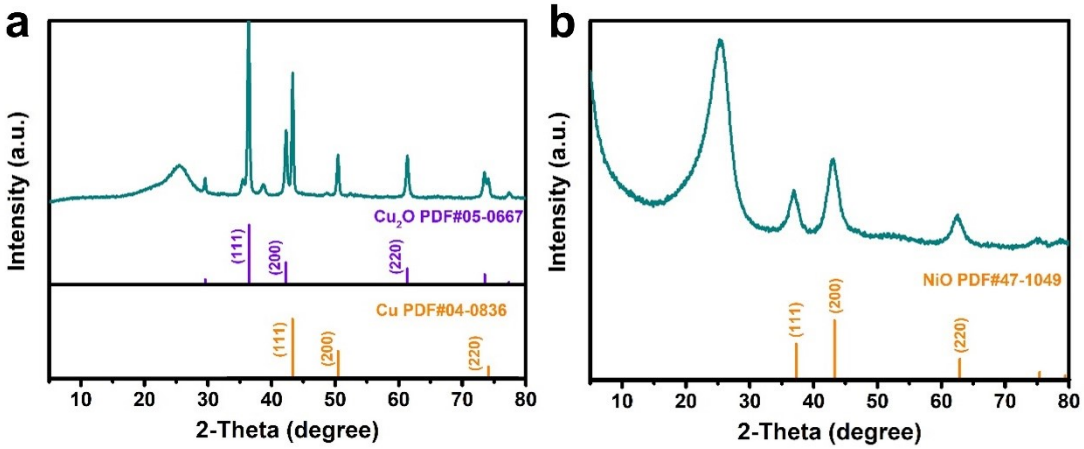

Fig. S5 XRD patterns of the CC@CuO_x (a) and CC@NiO (b).

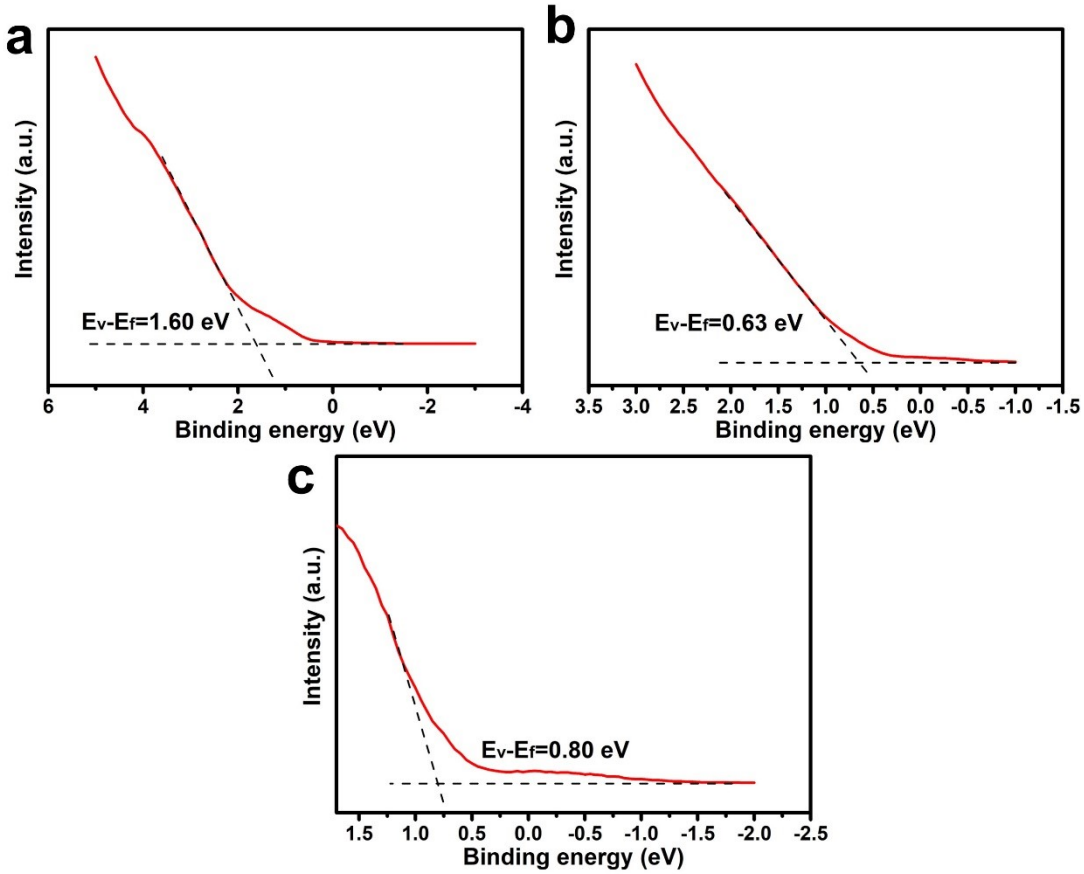

Fig. S6 Valence band curves obtained from the UPS spectra of the CC@NiO (a), CC@CuO_x (b), and CC@$NiCuO_x$ (c) electrodes.

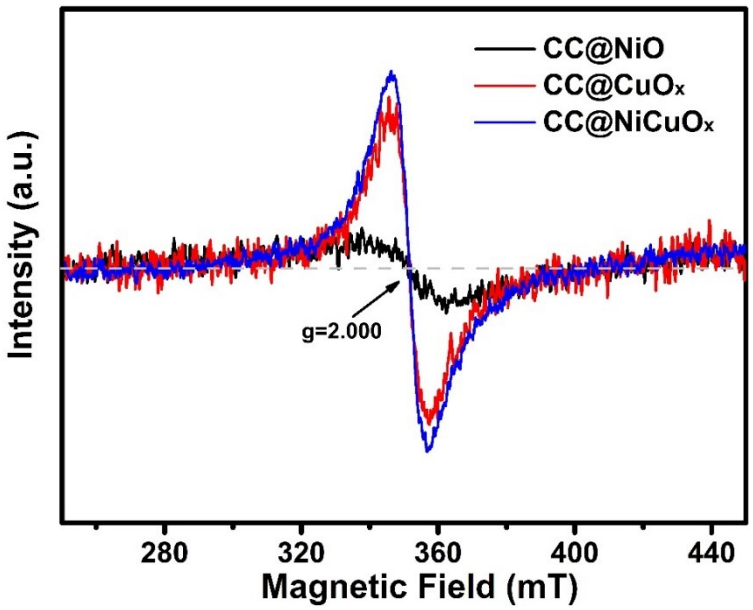

Fig. S7 Comparison of ESR results for the three samples.

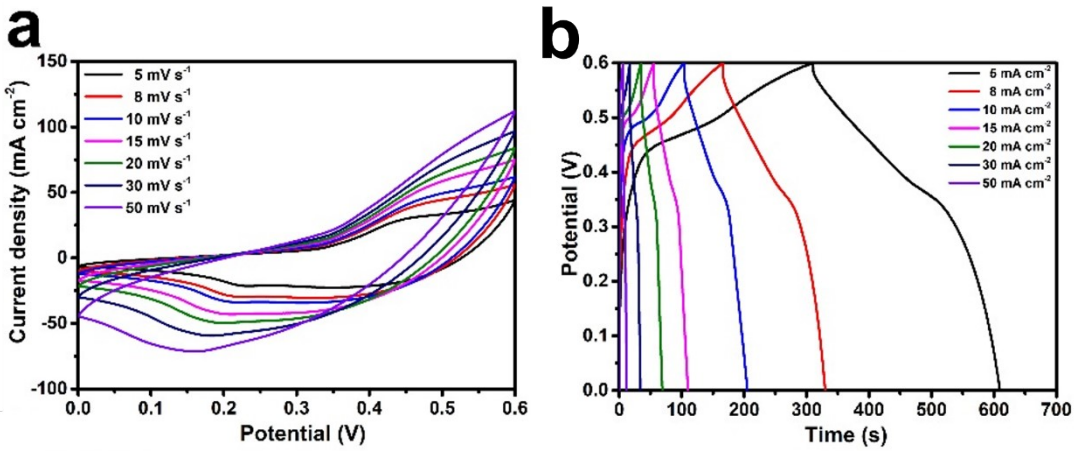

Fig. S8 CV curves obtained from various scan rates (a) with a potential window of 0-0.6 V (vs. SCE) and GCCD curves obtained from various current densities (b) of the $CC@NiCuO_x$ electrodes without light irradiation.

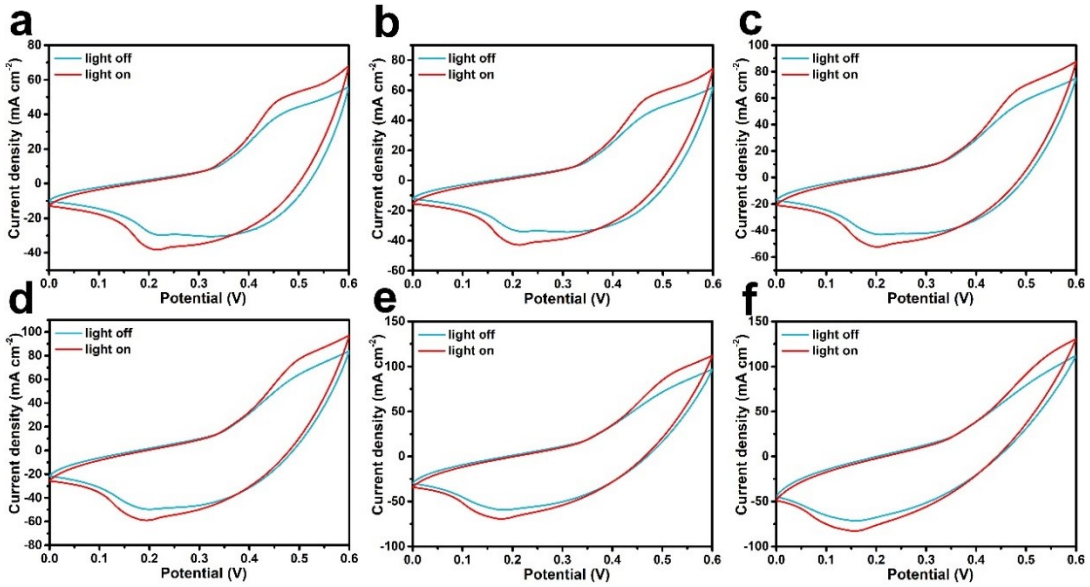

Fig. S9 Comparison of CV curves of CC@$NiCuO_x$ electrodes with light on/off conditions performed at specific scan rates of 8 mV s^{-1} (a), 10 mV s^{-1} (b), 15 mV s^{-1} (c), 20 mV s^{-1} (d), 30 mV s^{-1} (e), and 50 mV s^{-1} (f), respectively.

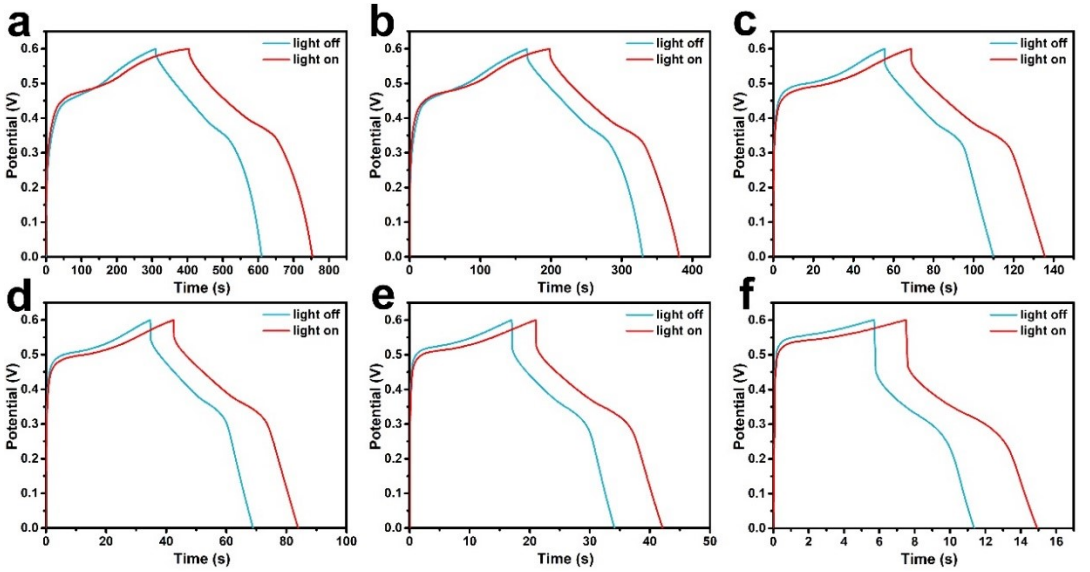

Fig. S10 Comparison of GCCD curves of CC@$NiCuO_x$ electrodes with light on/off conditions performed at specific current densities of 5 mA cm^{-2} (a), 8 mA cm^{-2} (b), 15 mA cm^{-2} (c), 20 mA cm^{-2} (d), 30 mA cm^{-2} (e), and 50 mA cm^{-2} (f), respectively.

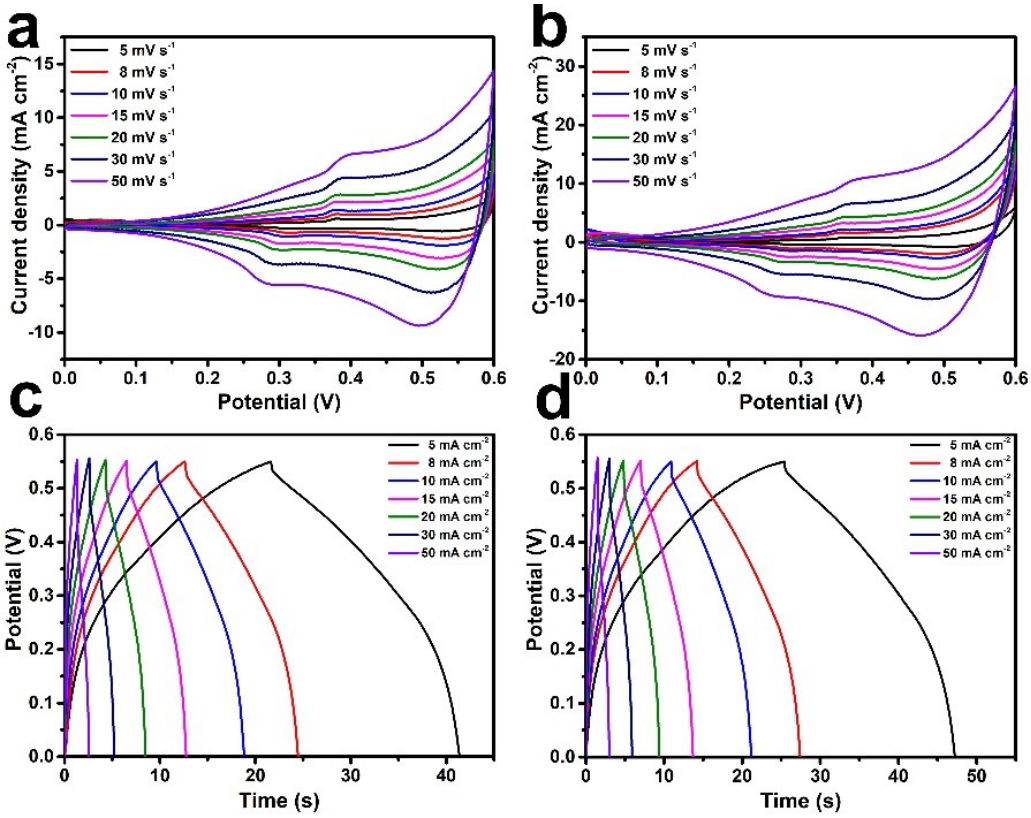

Fig. S11 CV curves (a-b) obtained from various scan rates with a potential window of 0-0.6 V (vs. SCE) without (a) and with (b) light irradiation, and GCCD curves (c-d) obtained from various current densities without (c) and with (d) light irradiation of the CC@CuO_x.

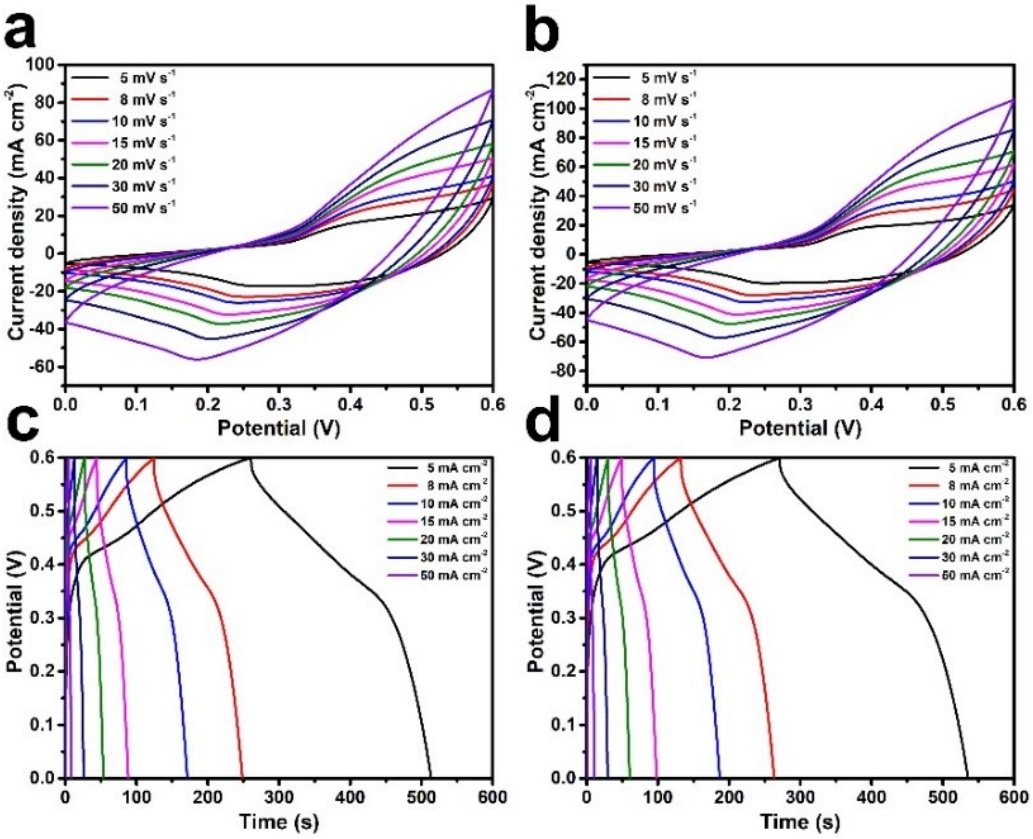

Fig. S12 CV curves (a-b) obtained from various scan rates with a potential window of 0-0.6 V (vs. SCE) without (a) and with (b) light irradiation, and GCCD curves (c-d) obtained from various current densities without (c) and with (d) light irradiation of the CC@NiO.

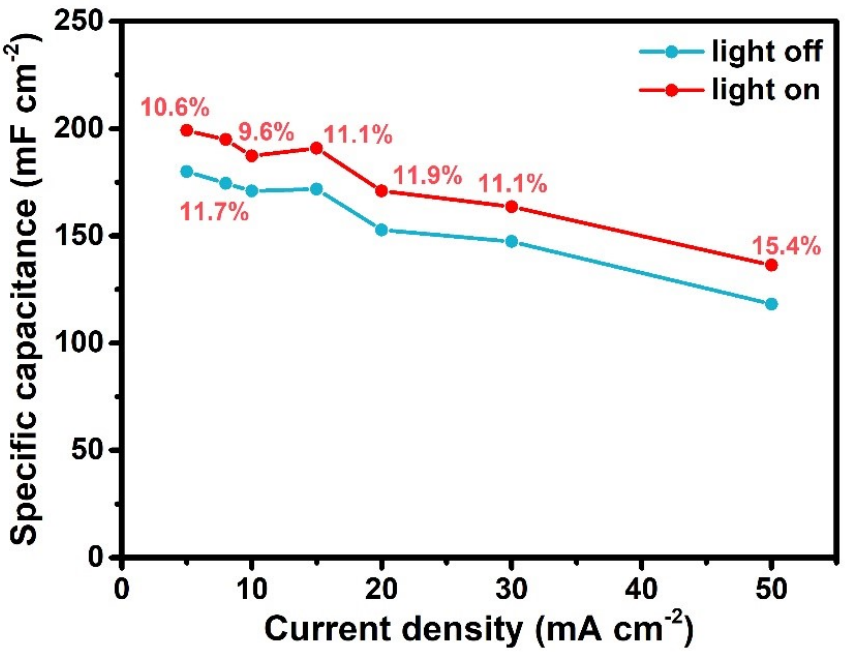

Fig. S13 Comparison of capacitance enhancements calculated at various current densities of the CC@CuO_x with light on and off conditions.

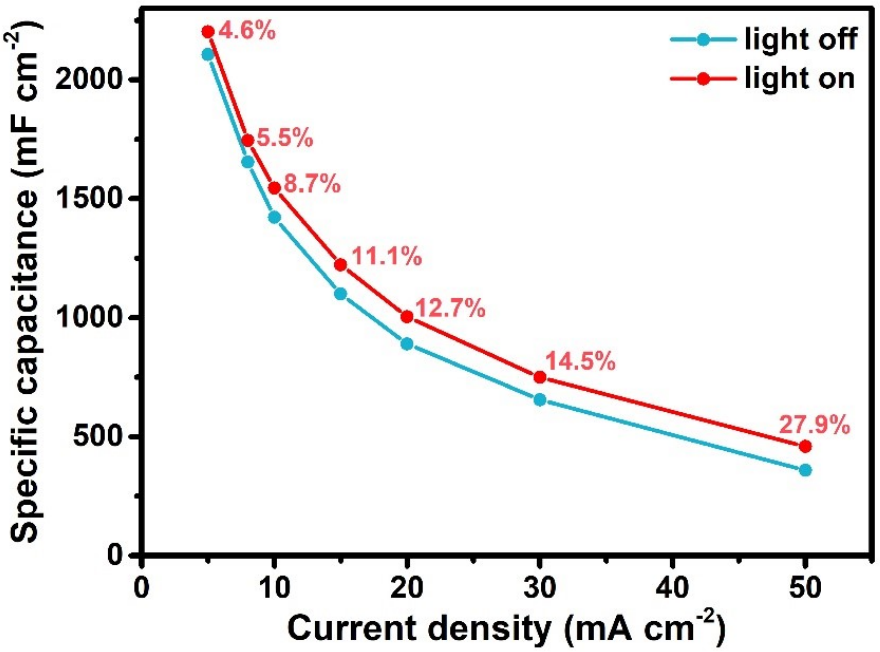

Fig. S14 Comparison of capacitance enhancements calculated at various current densities of the CC@NiO with light on and off conditions.

Table S1. Comparison of the as-prepared CC@$NiCuO_x$ bifunctional materials with other photoelectrodes for supercapacitors.

Photoelectrodes	Specific Capacitance	Stability	References
CC@$NiCuO_x$	2937 mF cm^{-2} at 5 mA cm^{-2}	~100% after 5000 cycles	This work
TiO_2/CNT fibers	0.6 mF cm^{-2} at 0.25 μA	/	1
TiO_2 nanotube arrays	1.1 mF cm^{-2} at 1 mA cm^{-2}	98.8% after 3000 cycles	2
Bi-polar TiO_2 nanotube arrays	262.5 mF cm^{-2} at 1 mA cm^{-2}	~90% after 5000 cycles	3
TiO_2/SNGP/CdS	104.6 mF cm^{-2} at 1 mA cm^{-2}	~85% after 5000 cycles	4
CF/TiO_2/MoS_2 fibers	18 mF cm^{-2} (1740 μF cm^{-1}) at 0.02 mA	~81% after 1000 cycles	5
PANI/CNT composites	422 mF cm^{-2} at 0.02 mA	~96% after 500 cycles	6
3D porous graphene and polypyrrole	2754 mF cm^{-2} at 0.5 mA cm^{-2}	85.8% after 10000 cycles	7
Indium tin oxide NWs	2.44 mF cm^{-2} at 0.02 mA cm^{-2}	93% after 10000 cycles	8

References

1. Angew. Chem. Int. Ed. 2012, 51, 11977-11980.
2. Adv. Funct. Mater. 2014, 24, 1840-1846.
3. Nano Energy 2018, 46, 168-175.
4. Nanoscale Adv. 2020, 2, 2925-2942.
5. Adv. Energy Mater. 2017, 7, 3, 1601208.
6. J. Mater. Chem A. 2017, 5, 23078-23084.

7. J. Mater. Chem. A, 2022, 10, 3382–3392.
8. ACS Appl. Mater. Interfaces 2021, 13, 22676−22683.